THE EFFECT OF SOFTENING ON THE BEARING CAPACITY OF MINE FLOORS

by

Gennaro G. Marino, Ph.D., P.E.[1] and Sung-Hoon Choi, M.S.[2]

Abstract. Based on analyzing case history data in the Illinois Coal Basin, it was determined that mine collapse resulting in surface subsidence can occur from floor softening. In other words, certain materials present in the mine floor can soften after coal extraction and fail when bearing pillars. The softening mechanisms considered are: 1. slaking/swelling due to moisture exposure, and 2. creep or strain softening due to sustained loads. In some case histories, the effect of floor slaking or swelling on floor stability is a fairly dramatic event by the occurrence of pooling of mine water and subsequent surface subsidence in the area of pooling. In other cases, the time factor is greater. The effect of softening on the ultimate bearing capacity of the mine floor was assessed by modeling representative conditions using FEM and elasto-plastic elements. In the models, the properties of softened mine floors were determined from results from subsurface exploration work in floor areas which were stable and others which had failed. The zone of softening was established on stress-field analysis.

Additional Key Words: floor stability, mine subsidence

Introduction

For vast areas underclay, clayey shale or claystone is present immediately below coal mined in the Illinois Basin (Odom and Parham, 1968). These non-durable floor materials are well indurated. Consequently, when these floors become saturated from pooling mine water there is a significant reduction in strength. Long-term creep also plays a role in softening the floor materials. In fact, based on the authors' observations the reduction in strength from floor softening can result in mine subsidence from pillar bearing failure. Marino et al, 1980 investigated the cause of a sag subsidence in O'Fallon, Illinois. Subsurface information indicated that water pooling had occurred on the mine floor and that yielding of the floor in bearing was the primary cause for mine collapse.

Also, mine floor failures resulting in surface subsidence continue to occur over post-1977 mines despite the use of state-of-art testing and floor bearing capacity analysis even where the extraction ratio was only 50%. Some practitioners and researchers believe, however, that mine flooding actually benefits stability as the water would assist in supporting the mine. In fact, in one case the authors are familiar with an abandoned mine in Illinois that was purposely flooded in order to provide additional support from the water. This action resulted in sags developing over the flooded section of the mine. Another erroneous theory which has continued to present time is that the hydrostatic pressure provided by the mine water provides confinement to the coal pillars.

In another study performed by Marino, et al 1982 and 1985 it was found that subsidence had occurred to approximately the limits of the mine pool. Outlines of these sags over the mine workings is shown in Figure 1. The effect of softening was indicated by moisture contents measured in the immediate floor. These moisture contents were found to be significantly greater in the rooms than beneath the pillars.

Mine failures and attendant surface subsidence can occur immediately to more than a half century after the time of extraction. The source of these time-related failures are mine rocks which are most susceptible to stress/strain and/or moisture deterioration. In other words, despite using conventional mine design methods, which assume initial rock strengths, the softening of non-durable rocks in the floor (as well as in the roof or pillar) cause these mines to fail resulting in turn in unplanned subsidence.

[1]Pres., Marino Engineering Associates, Inc., Urbana, IL

[2]Ph.D. candidate, Civil Engineering Department, University of Illinois, Urbana, IL

Proceedings America Society of Mining and Reclamation, 1998 pp 459-482
DOI: 10.21000/JASMR98010459

https://doi.org/10.21000/JASMR98010459

Failure Mechanism

The failure mechanism to be investigated in this paper involves failure of coal pillars in the Illinois Basin from mine floor softening based on the authors' observations. The most significant factors affecting the ultimate bearing capacity where the floor is susceptible to softening are given below.

- Material Softening Properties which depend on in situ strength properties, the deterioration potential (softened versus unsoftened strengths), strain softening characteristics, moisture sensitivity, sensitivity to cyclic moisture, lithology, and inherent and stress induced structure (mainly fissures).

- Confinement Stress which depends on pillar and room width, pillar load, depth below floor and horizontal location.

- Moisture Conditions which consist of moisture and cyclic moisture penetration into the floor both in the room as well as below the pillar.

These factors are discussed in detail in subsequent sections.

Although softening of floor rocks occurs from creep, significant deterioration also results from wetting (or wetting and drying) of non-durable materials. Consequently the time to bearing failure is many times strongly related to the time of floor saturation from pooling of groundwater and not an exponential time-function as would be thought from creep. The floor softening effect before failure initiates is conceptually depicted in Figure 2. Fundamentally, this softening of the floor reduces the component of bearing resistance from the passive wedge in the room and consequently the overall bearing capacity of the floor. This softening phenomenon is hardly considered in mine design today and is a major reason for continued subsidence events over abandoned as well as working underground mines.

From the authors' observation of over 75 cases of sag subsidence in the Illinois Basin mine failures generally occurred at lower average pillar pressures over time (see Figure 3). The two primary causes thought to cause these time-dependent failures are: 1. floor failure from softening, and 2. pillar failure from a yielding floor from softening.

The average pillar pressure values at 1 year or less have been plotted at 1 year and are quite scattered. The reason for failure in these scattered cases may be that the range of ground conditions for which these mines were designed were not representative of the conditions in failed areas, or the pillars were severely robbed with the reported extraction ratios then being inaccurate, or short-term floor softening from pooling of water or subterranean flow.

For 12 sag subsidence cases in the Illinois Basin where floor yielding or failure was suspected the strength of the underclay at failure was backcalculated (see Table 1). At each site listed in the table an extensive geotechnical investigation was conducted. Friction angles and undrained shearing strengths were backcalculated for long-term and short-term failures, respectively, using the relationships given by Mandel and Salençon, 1972. Mandel and Salençon considered a foundation resting on a ϕ,c material of limited thickness supported on a rigid base. The only undrained case considered is Case 1 (see Table 1) because an eyewitness account reported the failure occurred within a year as they were still moving equipment out of the area. No pooling was reported.

Assuming a negligible cohesion intercepts, friction angles were obtained for all the failures ranging from 21° to 31° (or friction coefficients of 0.38 to 0.60, respectively) with an average of 26°. It should be noted, as true with any back-calculated values at failure, the strength values reported in Table 1 are not necessarily the minimum or ultimate bearing strengths. They are only the values found at failure. These backcalculated friction values may be somewhat greater than the expected residual angles. Buffington, et al, 1980 found the residual friction angles for underclays from three different locations in the Illinois Basin to range from 9° to 22°. The underclays they tested had similar range in plasticity as those reported in Table 1.

Material Softening

Strain Softening

As mentioned above, material deterioration of rock results from both strain and moisture softening. Strain softening is defined as the reduction in the strength and stiffness due to load (whether the load is increasing, constant, or decreasing) with time without a change in the moisture content of the rock. Therefore this softening mechanism can be a drained or undrained phenomenon which results in fractures, joints and fissures. As a result of load induced destruction in clay shales the cohesion intercept can become negligible and the friction angle can become as low as the residual value.

Terzaghi et al, 1996 quantified the shear strengths of intact clay shales as a function of the overconsolidation ratio, OCR, an empirical coefficient, m, and the normally consolidated, reconstituted fiction angle. The equation of this relationship is:

$$s = \sigma' \tan\phi' [OCR^{1-m}] \qquad (1)$$

where σ' = the effective normal stress

m = 0.5 to 0.6

For destructured (with fractures induced by strain softening) shales m becomes 0.6-0.8. Considering an OCR of 25 for Illinois Basin underclays as reported by Marino et al, 1980 the likely strength reduction factor for the floor materials in question ranges from 0.38 to 0.72.

Moisture Softening

Moisture softening is the reduction in the strength and stiffness of the rock as a result of an increase in moisture content of the overall mass as well as locally along fractures. Exposure to free water has a significant effect on the strength of non-durable rock roofs and floors. The softening effect of water immersion on lab samples of argillaceous soils and rocks was tested by Morgenstern and Eigenbrod, 1974. These samples were tested in compression with 344.8 kPa [50 psi] confining pressure at their natural moisture contents and then at various transient stages until final "fully softened" values were reached.

Morgenstern and Eigenbrod's results indicated a significant loss of strength (60 percent of the initial value) occurred even when the slake durability rating was classified as little. Furthermore, the greatest strength losses occurred when the initial shear strength was less than 1,723.8 kPa [250 psi] with reductions to 5 percent of the unsoftened strength. Another interesting observation made by Morgenstern and Eigenbrod was that of all the samples tested, soft to hard sandstones and shales/mudstones took the longest time to reach their fully softened state.

An important assessment in predicting the extent and degree of softening of mine floors is to determine the rock durability. For example a completely durable rock zone, such as a cemented sandstone or a limestone, there would be little loss in strength from exposure to water. Consequently for these materials it is not necessary to consider the effects of changes in moisture in the mine environment when performing floor stability calculations for most situations. Many classification systems based on lab-derived indexes properties have been developed to differentiate varying degrees of rock durability. These classification systems are typically used to predict roof behavior. The capacity of the rock to span openings, however, requires a much more harsh criteria than is needed in floor bearing of pillar loads. For other classifications such as by Deere and Gamble, 1971 the slake durability classification appears too general for the purpose of estimating floor softening.

The most difficult materials to classify are shales because of their wide range of engineering properties. For the purpose of assessing rock durability in floor bearing capacity calculations the parameter termed the Durability Rating, DR_S, may have potential. This term DR_S was developed by Richardson and Wiles (1990) for shale materials. They described shale as "any geologic material that is an indurated, nonmetamorphosed sediment composed mainly of clay and silt. Shale will thus include siltstones, mudstones, mudshales, claystones, clayshales, arenaceous shales, siliceous shales, bituminous shales, and gypsiferous shales."

The Durability Rating is defined as follows:

$$DR_S = 100 - \Delta S_R \qquad (2)$$

where:

$$\Delta S_R = \frac{\left(\frac{\sigma_1}{\sigma_3}\right)_{ps} - \left(\frac{\sigma_1}{\sigma_3}\right)_{pw}}{\left(\frac{\sigma_1}{\sigma_3}\right)_{ps}} X\, 100 \qquad (3)$$

where: ΔS_R = the change in shear strength as determined by peak stress ratio, %; $(\bar{\sigma}_1 / \bar{\sigma}_3)_{ps}$ = the peak stress ratio of a silicon test, average of 3; and $(\bar{\sigma}_1 / \bar{\sigma}_3)_{pw}$ = the peak stress ratio of a water test, average of 3. ΔS_R is basically a strength loss parameter due to water saturation and subsequent deterioration of the shale

Richardson and Wiles performed triaxial tests on 10.2 cm. (4 in.) diameter, 20.3 cm. (8 in.) long compacted shale samples with the individual shale particles less than 1.9 cm. (3/4 in.) in size. Although the above classification was based on triaxial testing of shale particles this simple classification approach appears to have potential for intact shale samples.

The following equation was developed to relate DR_S to index properties.

$$DR_S = 61.6 + 0.3488(I_{SD2}) - 2.1562(NMC) \qquad (4)$$

where: DR_S = durability rating, based on shear strength loss, from 0 (least durable) to 100 (most durable); I_{SD2} = sieved slake durability index[3], %; NMC = natural moisture content, %.

If the sieved slake durability index is not available DR_S can be determined from the conventional 2-cycle slake durability test results by:

$$I_{SD2} = 7.269e^{0.0273 I_{D2}} \qquad (5)$$

where: I_{D2} = 2-cycle slake durability, 10 min, 200 revolutions each cycle, %.

Equation (3) can be written as:

$$DR_S = 61.6 + 2.5354e^{0.0273 I_{D2}} - 2.1562\ (NMC) \qquad (6)$$

Richardson and Wiles classify shales based on DR_S as given in Table 2. Based on this classification a DR_S of 70 or greater may be appropriate for determining materials which will only undergo limited amounts of weathering. The advantage in using the above criteria is that it is only necessary to determine the natural content and the slake durability of the shale to obtain a feeling for the weatherability of shale-like floor materials in terms of loss in strength.

---

[3]The sieved slake durability index is a cumulative weighted percentile based on the 2-cycle gradation of the rock (Richardson and Long, 1987).

Figure 4 shows the relationship between 2-cycle slake durability index and natural moisture content for shale-like roof and floor materials from an Indiana coal mine DR_S values of 50%, 70%, and 90% are depicted on Figure 4 from Richardson and Wiles' relationship (Equation 4) in order to discern areas of different durability classification. As can be seen in Figure 4, the material characteristics of the data appear to correspond fairly well with expected durability based on lithologic descriptions. Consequently, from this comparison sufficiently durable rocks might be considered with a DR_S of 70% or greater.

Stress Distribution in the Floor

Closed-form elastic relationships were used to access the stress distribution in the floor below the room (Poulos and Davis, 1974). Uniform loading over square to infinite strip areas were considered in assessing the vertical stress distribution in the floor.

The distribution of vertical stress is calculated in terms of the Original Stress Ratio, OSR. The parameter OSR is used as a measure of rebounding potential by comparing the vertical loading on a floor element before and after mining. OSR is determined as follows:

$$OSR = \frac{\sigma_z + \Delta\sigma_{pt}}{\sigma_{vo}} \qquad (7)$$

where: $\sigma_z = \gamma d_f$ = total vertical stress on element below room

$\sigma_v = \gamma D$ = original total vertical stress of rock on element

As shown on Figure 5, for strip pillars the OSR lines with d_f/W_r (where W_r = room width) for points below the middle of the room are essentially independent of D/W_r = 10 to 1,000 (or in other words independent of the magnitude of pillar load). Also, for both the strip and square pillar cases the distribution of OSR with relative depth (d_f/W_r) below the room at mid-pillar were found to be identical (see Figure 6). These identical stress distributions further indicated that the OSR contours in the room are independent of pillar width, W_p. Therefore, as for strip pillar (or narrow pillar) OSR for square pillars is essentially independent of depth and D/W_r.

Although beneath the pillar OSR is greater than one, in the room OSR was not found to approach unity until the relative depth (d_r /W_r) reached 3.0 to 4.0 for extraction ratios of 50% to 30%, respectively. At d_f /W_r equal to 0.5 the range in OSR values in the middle of the room are only from about 0.25 to 0.32 for E from 30 to 50%, respectively. However, the lower the extraction ratio (E) the shallower and flatter the bottom of the OSR contours are below the room. This can be seen from Figures 7 to 9. Furthermore, for the extraction ratio considered there is not a significant difference in the OSR in the immediate floor.

At the middle of room intersections, for a square pillar configuration as can be seen in Figure 10 OSR only ranged from about 0.08 to 0.14 for $d_f /W_r = 0.5$ with E ranging from 30 to 50% respectively. These OSR values are about 35% those for the strip case and mid-square pillars. The reason for this is basically the greater diagonal distance to the mid-point in a room intersection compared to the middle of the room. To achieve the same range of OSR as in the strip or mid-square pillar case (i.e. 0.25 to 0.32) at d_f /W_r at 0.5 a relative depth of $d_f /W_r = 0.8$ must be reached.

In the room intersection of a square pillar geometry, as shown on Figures 11 to 13 the bottom of the OSR contours does not appear to change significantly across the room with extraction ratios from 30 to 50%. However, for strip to mid-rectangular/square pillars the bottom of the contour appears to be flatter with lower E values.

Although not included in this report the same OSR study as above was done for extraction ratios of 60 and 70%. Similar trends were found, however, OSR became greater than one near the pillar edge for both the strip and square pillar configurations. For both the strip and square cases the greatest OSR reaches 1.75 at the pillar edge for an extraction ratio of 70%. Also for extraction ratios of 60 and 70% the OSR values for 1/8 points and edge are greater for the square pillars. This difference appears most pronounced from about a d_f /W_r of 0.5 to 1.5.

The Extent and Degree of Moisture Softening

The extent of floor softening as postulated herein can be seen by comparing floor moisture contents with depth from under the pillar and below the room. This type of data was taken in two case histories where the mines had been abandoned for some time (Marino et. al., 1980, and Marino et. al., 1982, and Marino and DeVine, 1985). A summary of the moisture data is given in Figure 14 and Table 3. What can be seen from this data is summarized below.

1. There appears to be a significant difference in the natural moisture content in the immediate floor below the room and below the pillar. This difference in the immediate floor appears to become less closer to the center of the pillar.

2. Moisture content profiles in Figure 14 indicate that the obvious difference in moisture contents below rooms and pillars decrease and approximate zero at some depth.

3. The depth to approximate zero moisture change appears to be related to the location of a more durable rock zone below the underclay/claystone.

4. The immediate floor in the rooms was found to be very soft.

5. Suspect softened zones in room at intermediate depths as a result of bed separation from rebound and subsequent swell of localized non-durable rock layers. This condition is depicted as moisture anomalies at 2.13 and 3.66 m in Figure 14.

Figure 15 is a plot of swelling pressures plotted against the existing overburden pressure for a number of shale samples with different moisture contents, plasticity, clay content and overconsolidation ratios. The figure indicates that the odemeter swell pressures measured in the laboratory generally increase with depth and appear to approximate the total overburden pressure. Exposing the sample to free water during the odemeter test is similar to mine flooding. Therefore an increase in moisture content in the floor can be assumed to ultimately occur to a depth where an OSR of one is reached.

One condition which may not be representative of the field condition would be the initial void ratio of which the swell test is performed. The difference between the lab initial void ratio and that in the field is the result of material rebound and the development of stress relief microfractures. A sample less compressed than the field condition will result in lower swell pressures measured.

Figure 15 indicates that with the presence of free porewater the potential for swelling exists in some shales even when there is no difference in confining stress (e.g. OSR equal to one). The amount of swelling strain or softening based on laboratory tests is, however, small. Laboratory tests indicate that even at OSR values of 0.10 or less (free swell) the strains are still typically small.

These laboratory swell measurements appear contrary to field conditions based on the data presented in Figure 16 and Table 3 as well as the observable factor that floor failure can be incited by mine pooling. Backcalculated swelling strains versus OSR are plotted in Figure 16. Swelling strains were backcalculated from Figure 14 by considering the initial moisture contents were those measured beneath the pillar and the final values those measured in the room, and assuming saturated conditions. As can be seen in Figure 16 significant swell strains have been estimated. The difference in the anticipated swell strains from laboratory measurements and those backcalculated from field data may be due to duration of the lab tests (days) versus field (years to over 100 years).

Rate of Moisture Softening

Laboratory values from odemeter testing on the rate of hydrodynamic swelling such as given by Cepeda-Diaz 1987, result in very large unrealistic times to reach a fully softened state. There is an obvious discrepancy in the rate of softening predicted from theory using average laboratory measurements assuming that mine water is available. From observation, after pooling of water floor failures in non-durable materials can occur fairly rapidly in a matter of months to years. Furthermore, plate bearing tests performed on Illinois underclay/claystone floors after being soaked for only 24 hrs have shown a decrease in plate bearing of up to 50% (Chugh, 1990). For floor underclays-claystones in the Appalachian coal field it was not uncommon to find when performing rapid plate bearing tests that one-half of the unsoaked strength would be lost after short-term soaking (Peng, 1986).

In situ factors which significantly affect the rate of softening are: 1. increases in the rock mass permeability as a result of stress relief fractures, as well as inherent fissures and joints; 2. increases in the rock mass permeability as a result of any slake-induced micro-fracturing; 3. the supply of groundwater from underlying more permeable rock strata (which may act alone without pooling mine water); and 4. the one-dimensional rebound for some shale samples tested in the lab showed coefficients of swelling at 2,000 times higher rates at the highest OCR compared to lowest OCR values tested (Cepeda-Diaz, 1987). (It should be noted, however, that some of the shales tested showed completely the opposite trend.)

Although "immediate" softening is significant enough to cause "rapid" floor failures this does not mean that a fully matured softened zone was present. This is particularly true for thick non-durable floors where the rate of softening with depth is apt to be significantly longer due to less fracturing and significantly lower in situ coefficients of swelling at lower ranges of OSR as stated above. Furthermore, long-term secondary (after primary) swelling must be considered in the evaluation of ultimate softening for more deep-seated conditions as well as in the immediate floor (Terzaghi et. al., 1996).

In one study it was found that about 40 years was required to dissipate the negative pore pressures which resulted when the slope of a highly overconsolidated fissured clay was cut. This data as shown in Figure 17 indicates that after 20-30 years much of the swelling had resulted.

More rapid rates of moisture softening is also indicated by the moisture data presented in Figure 20 and Table 3. These moisture contents measured in the rooms were taken 20 years or less after coal extraction.

The Effect of Softening on the Ultimate Bearing Capacity

Estimation of Softened Zone in Rooms

By assuming certain softening conditions the effect floor softening has on the ultimate bearing capacity can be determined by numerical analysis. In this study the eventual condition of saturation of the mine floor from the pooling of groundwater is assumed.

Based on the available data given in Figure 16 the amount of softening which can occur in situ can be projected. Using this data Table 4 was compiled. The table compares the amount of estimated vertical swell strain the immediate floor had undergone to the respective OSR value at a distance of 0.25 times the room width (i.e., OSR at 1/4 point). The 1/4 Pt OSR was determined for each moisture content taken in the immediate floor based on the depth of the measurement and on the specific extraction ratio and width room based on the mine map.

The vertical swell of the floor in the rooms was determined by comparing the measured moisture contents in rooms to the moisture contents below the pillar at the same relative depth. Borings B-5 and B-6 provided moisture data in rooms and Boring B-1 was used for under the pillar (see Figure 14). The vertical swell strain, ϵ_v, was estimated from the following equation:

$$\epsilon_v = \frac{e_f - e_0}{1 + e_0} \qquad (8)$$

where: e = void ratio = (MC*G) /S

S = saturation level = 100% (assumed)

e_0 = initial void ratio

G = specific gravity of grains =2.7 (assumed)
e_f = final void ratio

MC = moisture content (%)

To obtain a feeling for the degree of swelling required to approach a fully softened state a well known equation developed by Speck, 1979 can be used.

$$Q_u = 14272.6 - 1151.5MC \qquad (9)$$

where: Q_u = compressive strength (kPa)

The underclays and claystones studied by Speck had similar moisture and plasticity properties as those floor materials used in this analysis.

For fully softened samples tested in uniaxial compression the development of negative porewater pressures from rebound or shearing is mostly likely negligible. As no normal stresses will exist to speak of, because of nominal porewater pressures, the frictional contribution to the resulting fully softened compressive strength will be small, if any. Therefore the only strength component which will largely determine uniaxial compressive strength in the fully softened state will be from presence of any remaining cohesion intercept of the material.

Using Equation (9) the compressive strength is found to equal zero at a moisture content of 12%. Or in other words, the undrained cohesive strength (and thus the effective cohesion intercept) accumulated from induration can be thought to be reduced to zero and the softened shear strength could be assumed to be based on only the underclay/claystone's fully softened friction angles. Skempton 1964, and 1970 found that the long-term strength of slopes cut in London Clay, which were then exposed to weathering, best correlated with the fully softened or critical state strength of the material. London clay is a highly indurated (overconsolidated) clay containing fissures and behaves similarly to clay shales. Where large shear strains had occurred, however, this shear strength of these highly overconsolidated clay would reduce to its residual value.

A sensitivity analysis considering different initial (but typical) moisture contents in the floor ranging from 5% to 8% indicate critical swell strains of 17% to 9%, respectively, are necessary to obtain a final moisture content of 12%. Consequently, a 10% swell strain can result in the most immediate floor materials (in the room) becoming fully softened and reducing to residual strength levels as a result of significant fissuring.

To determine the OSR value corresponding to a 10% swell, the ϵ_v and OSR (1/4 pt) data given in Table 4 has been plotted in Figure 16. As can be seen in this figure the amount of swell varies with the estimated OSR. The foremost influence on the range on swell is probably related to the heterogeneities in the floor such as the presence of partial cementations, limey concretions and the clastic content. In other words the extent of softening within the non-durable floor zone will vary. Assuming the rock mass strength will be actually determined by the most softened areas a maximum swell line is used to assess the OSR value which corresponds to the fully softened swell value of 10%. This line as plotted in Figure 16 indicates that fully softened conditions can be assumed when an OSR of 0.45 or less is present.

Based on Figures 7 to 9 for both strip and square pillar configurations d_f/W_r ranges from 0.46 to 0.60 for extraction ratios of 50% to 30% respectively, for an OSR (1/4 pt) of 0.45. Therefore, in the numerical analysis performed below a fully softened condition is assumed in the room to a d_f/W_r of 0.5. Of course, in situ there is no discrete boundary between fully softened and unsoftened materials. However, for this analysis it is assumed that a softening transition zone does not significantly affect the results.

Strain Softening in Floor

As mentioned earlier, softening of the floor occurs as a result of strain softening as well as from slaking and swelling. Terzaghi et al, 1996 reported that where significant fissuring is present, clay shales essentially lose their cohesion and maintain only a residual shearing strength. In underclay floors fissuring can be assumed present and will develop further from mining

In order to develop load induced fractures from mining, critical shearing strains must develop. As the pillar loads increase critical shearing strains in the room as well as under the pillar will develop. As a result, the shearing resistance and stiffness of the floor materials reduces even without any significant change in moisture.

Assumed Properties for Floor Material

Three different stress-strain states were assumed in the subsequent bearing capacity analyses for the underclay/claystone floor. These are: intact-unsoftened; destructured; and residual-fully softened. The major input materials parameters required to perform this stability analysis were Young's Modulus, Poisson's Ratio (assumed equal to 0.3), and the friction angle (with the cohesion assumed to equal zero).

For this analysis field Young's modulus values were taken from those recommended by Hendron et al, 1969. Based on the modulus data measured on shales in the Illinois Basin the following empirical relationships were developed.

For "gray shale"

$$E_M = 1.717X10^6 \; 10^{\frac{-MC}{6.133}} \tag{10}$$

For "black shale"

$$E_M = 9.86X10^6 \; 10^{\frac{-MC}{6.36}} \tag{11}$$

where: E_M = field Young's Modulus, kPa

The "gray shale" is reported by Hendron, et. al., 1969 to have properties similar to underclay/claystone in question in this study. The stiffness of the lower floor shale unit is assumed to be equivalent to the "black shale", whose modulus is about an order of magnitude greater than the "gray shale". It is interesting to note that when applying Equation (10), Young's Modulus in the floor is 6.5 times greater under the pillar than in the room even when considering only a 5% difference in moisture contents between the two areas.

Intact-unsoftened state was considered uniformly present in the underclay/claystone before any stress or moisture induced softening results. The unsoftened material strength properties of the underclay/claystone were determined by the critical state condition. The unsoftened state was also assumed under the core of the pillar when material deterioration was considered in the rooms and along the perimeter of the pillar.

As stated by Bertocci et al, 1995, the residual and critical state strengths of clay shales are solely dependent upon the compositional characteristics of the material regardless of their fabric and structure. The critical strength is determined in the lab from normally consolidated reconstituted samples. Both critical state as well as residual strength are cohesionless and therefore are only related to a friction angle.

Based on the plasticity characteristics of the underclay/claystone in question and the relationships given by Cepeda-Diaz, 1987, a critical state friction angle of 30° is assumed. To determine Young's Modulus for the stress-strain state Equation (10) was applied using a moisture content of 7%, or in other words a modulus value of 124,482 kPa [18,054 psi] was assumed.

Once sufficient shear strains developed from loading a destructured zone of the underclay/claystone floor was considered beneath the perimeter of the pillar and under the residual fully softened floor in the room (when lower and stronger shale was not present). In this zone no moisture content increase is considered, however, the modulus was reduced to 50% of the intact value based on the affect destructuring has on the strength. Also because of the inherent and load-induced fissures, high shear strains, and plastic properties, a residual friction angle of 15° was assumed. It was assumed that destructuring of the underclay/claystone resulted when a shear strain of 8% had been reached.

The residual-fully softened state is defined by floor material which has been completely moisture and strain softened. Consequently a residual friction angle of 15° are assumed and a Young's Modulus of 8,963 kPa [1,300 psi] (based on Equation (10) using a moisture content of 14%). The selected residual friction angle of 15° is based on empirical correlation between the liquid limit and clay fraction of the material to the residual friction angle developed by Stark and Eid., 1994. A liquid limit of 50% (ball-milled, minus #200 sieve) and a clay fraction of greater than 45% was assumed for the underclay/claystone.

This residual-fully softened zone was assumed to extend across the room and be present to a depth of one-half the room width or to the depth of the underlying durable shale, whichever was less. The assumed durable shale immediately below the underclay/claystone layer is considered to have a friction angle of 40°, cohesion of zero, and a Young's Modulus of 1,123,244 kPa [162,907 psi].

Modeling Conditions

In order to determine the effect of floor softening on the ultimate bearing capacity of the floor both softened and unsoftened cases were analyzed. To model the floor strata the FEM program called SMAP-2D developed by COMTEC was used. A sample mesh which contained plane strain, isoparametric 4-node elements, is shown in Figure 18. These non-linear elastic-plastic elements were defined by their elastic and Mohr- Coulomb properties such as given above.

The 2-dimensional model was varied by keeping the room width constant at 6.1 m. [20 ft.] and changing the size of the pillars. Trials were run at W_p /W_r of 1.0, 2.5, and 5.0. Also, for each W_p /W_r ratio, W_p /h_1 was varied from 1 to 10 (where h_1= underclay/claystone thickness). The underclay/claystone however, was limited in the thickness to three times the room width (in other words 18.3 m. [60 ft.]).

The loading was applied to the floor by incrementally and uniformly displacing the pillar areas downward. For each increment of displacement the average vertical pillar stress was determined from the floor elements immediately below the pillar.

Effect of Softening on the Ultimate Floor Bearing Capacity

In order to study the effect of softening on the ultimate floor bearing capacity pillar bearing pressures at failure were determined for both unsoftened and softened cases. These results were then compared by determining the reduction in bearing due to softening. This was quantified by calculating the Reduced Bearing Capacity Ratio, RQR, which is the unsoftened bearing capacity divided by the unsoftened value. The ultimate bearing capacity was determined by the maximum average pillar bearing pressure at the vertical displacement of 15.2 cm. or less.

The RQR was found to vary with W_p /W_r and W_p /h_1 with the assumed material properties stated above. Based on the FEM results the relationship of RQR to various W_p /W_r and W_p /h_1 values is given in Table 5.

As can be seen from Table 5 the RQR was found to vary from as low as 14% to 57%. For mining geometries that are presently used W_p /W_r of 2.5 and 5.0 are more appropriate. For these ratios the RQR ranged from 31% to 57%, or in other words based on the assumptions made in this paper, the ultimate floor bearing capacity in the softened state can be expected to be as much as 2 to 3 times less than the unsoftened or short-term capacity.

Also, for some extraction ratio (or a constant W_p /W_r), the lowest RQR is found where the softened depth in the room equals the total thickness of the underclay/ claystone (i.e. $W_p /h_1 = W_r /2$). In this study a room width of 6.1 m was assumed.

From the trial cases run it was found that a softened floor in the room would result in progressive failure of the underclay/claystone layer. Basically the reduced floor strength and stiffness (as a result of strain and moisture softening) in the room significantly affected the amount of passive wedge resistance which can be generated at the pillar perimeter. This failure is consistent with the perimeter bearing failure mechanism postulated by Marino et al, 1980 where pillar failure was suspected 19 years after coal extraction. An example of the formation of these inward progressive slips is shown in Figure 19. Figure 19 is a contour plot of the octahedral shear strain at the time of first slip at the pillar perimeter. (Note the critical shear strain was considered to be 8%). Also it can be seen from the contour map that the interior portion of the underclay/claystone floor has remained elastic. This is also demonstrated by a plot of the vertical bearing pressure along the pillar which is depicted in Figure 20 for the example case shown in Figure 19.

After each progressive slip another trial was run until complete bearing failure was obtained. Before the performing the next trial the previous slip zone was assumed to be destructured. With increased deflection of the pillar additional slips occur inward towards the core of the pillar. As this failure process continues the width of elastic core of the floor reduces and the pillar settlement becomes excessive even though the sustained load may increase. Failure was considered when the maximum load was reached or the pillar deflection eqnaled 15.2 cm. [6 in.]

Literature Cited

Bertocci, P., Canuti, P., Casagli, N., Garzonio, C.A. and Vannacci, P., 1995. Landslides on Clay and Shale Hillslopes in Tuscany, Italy, AEG Reviews in Engineering Geology, Volume XS, Clay and Shale Slope Instability, pp 107-119.
https://doi.org/10.1130/reg10-p107

Buffington, D., Stephenson, R. W., and Rockaway, J. D., 1980, Residual Strength of Underclay, 21st Symp. on Rock Mechanics, U. of Missouri - Rolla, pp. 435-445.

Cepeda-Diaz, A. F., 1987, An Experimental Investigation of the Engineering Behavior of Natural Shales, Ph.D. Thesis, Dept. of Civil Eng., U. of Illinois, 692 pp.

Chandler, R.J. 1988, The In Situ Measurement of the Undrained Shear Strength of Clays Using the Field Vane, Proc. Int. Symp. on Vane Shear Strength Testing in Soils: Field and Laboratory Studies, ASTRM STP No 1014, pp 13-44.

Chugh, Y. P., 1990, Workshop on Design of Coal Pillars in Room-and-Pillar Mining, Dept. of Mining Engineering, Southern Illinois University, Carbondale, 71 pp.

Deere and Gamble, 1971, Durability-Plasticity Classification of Shales and Indurated Clay, Proc. 22nd Annual Highway Geology Symposium, University of Oklahoma, Norman, Okla., pp. 37-52.

Fleming, R. W., Spencer, G. S., and Banks, D. C., 1970, Empirical Study of Behavior of Clay Shale Slopes, Vol. 2, NCG Technical Report No. 15, AD-729 849, 301 pp.

Hendron, A. J., Mesri, G., Gamble, J. C., and Way, G., 1969, Compressibility Characteristics of Shales Measured by Laboratory and In Situ Tests, ASTM Winter Meeting on Determination of The In Situ Modulus of Deformation of Rock.

Mandel, J., and Salençon, J., 1972 Force Portante d'un Sol Sur une Assise Regide Etude (Theoretique), Geotechnique, Vol. 22, No. 1, pp. 79-93.
https://doi.org/10.1680/geot.1972.22.1.79

Marino, G. G., Mahar, J. W., Cording, E. J., Shively, J. E., and Lundin, T. K., 1980, Mine Subsidence and Related Damage in O'Fallon, Illinois, AMLRC Phase II Report, 100 pp.

Marino, G. G., Mahar, J. W., Dobbels, D. J., and Kiesling, D. R., 1982, Mine Subsidence and Related Structural Damage, Hegeler, Illinois, Final Report for USBM, 120 pp.

Marino, G. G., and Devine, A., 1985, Mine Subsidence and Structural Damage, Hegeler, Illinois, from July, 1981 to February 1982, USBM Report, 45 pp.

Marino, G. G., 1990, Progressive Failures of a Danville Area Room and Pillar Mine and a Comparison to other Illinois Mine Failures, 9th Int'l Conference on Ground Water Control in Mining, Morgantown, WV.

Marino, G. G., and Bauer, R. A., 1990, Behavior of Abandoned Room and Pillar Mines in Illinois, Int'l Journal of Mining and Geological Engineering, 11 pp.

Morgenstern, N. R., and Eigenbrod, K. D., 1974, Classifications of Argillaceous Soils and Rocks, ASCE, Jrn., GT10, pp. 1137-1156.

Odom, I. E. and W. E. Parham, 1968, Petrography of Pennsylvanian Underclays in Illinois and Their Application to Some Mineral Industries, IL State Geological Survey, Circular 429, 36 pp.

Peng, S. S., 1986, Coal Mine Ground Control, 2nd edition, John Wiley and Sons, Inc.

Poulos, H. G., and Davis, E. H., 1974, Elastic Solutions for Soil and Rock Mechanics, John Wiley and Sons, NY, 411 pp.

Richardson and Long, 1987, The Sieved Slake Durability Test, Bulletin of the Association of Engineering Geologists Vol. XXIV, No. 2, pp. 247-258.

Richardson and Wiles, 1990, Shale Durability Rating System Based on Loss of Shear Strength, Geotechnical Engineering, pp. 1864-1880.

Speck, R. C., 1979, A Comparative Evaluation of Geologic Factors Influencing Floor Stability in Two Illinois Coal Mines, Ph.D. Thesis, University of Missouri, Rolla, 265 pp.

Skempton, A. W., 1964, Long-term Stability of Clay Slopes, Geotechnique, 14, No. 2, pp. 77-101.
https://doi.org/10.1680/geot.1964.14.2.77

Skempton, A.W., 1970, First-time Slides in Over-Consolidated Clays, Technical Notes, Geotechnique, Vol. XX, No.3, pp. 320-324.
https://doi.org/10.1680/geot.1970.20.3.320

Skempton, A.W., 1977, Slope Stability of Cuttings in Brown London Clay, Proc. 9th Int. Conf. on Soil Mech. and Found. Eng., Tokyo,3, pp. 261-270.

Stark, T.D. and H.T. Eid, 1994, Drained Residual Strength of Cohesive Soils, J. Geotech Eng., ASCE, 120 No. 5, pp 856-871.

Terzaghi, K., Peck, R. B., and Mesri, G., 1996, Soil Mechanics in Engineering Practice, 3rd Edition, John Wiley and Sons, Inc.

TABLE 1 BACKCALCULATED UNDRAINED SHEAR STRENGTH AND FRICTION ANGLES AT FAILURE FOR SUBSIDENCE CASE HISTORIES IN THE ILLINOIS BASIN (MARINO, 1990)

SAG NO.	ESTIMATED PILLAR PRESSURE kPa	YEARS TO FAILURE	ESTIMATED AT FAILURE S kPa	ESTIMATED AT FAILURE ϕ, c=0	UNDERCLAY PLASTICITY LL %	UNDERCLAY PLASTICITY PI %
1	2,889	1	579		48-51	21-28
2	3,447 i 4,716 f	4		27°		
3A	3,089	15		26°		
3B	3,000 i 3,447 f	(15) 17		21°		
4	3,041 i 3,834 f	(15) 18		31°		
5	2,517 i 3,392 f	(20) 20		27° *		
6	2,420 i 2,634 f	(15)		30°		
7	2,331 i 4,716 f	(15) 20		21°		
8	3,530	60		21°	49	31
9	1,931	<33		23°		
10	3,385	19		22°	36-43	11-19
11	1,931	20-69		24°		

S = undrained shear strength
ϕ = friction angle
c = cohesive intercept
LL = Liquid Limit
PI = Plasticity Index
i = initial
f = final

* soft immediate roof materials may have contributed the bearing failure

TABLE 2 SHALE DURABILITY CLASSIFICATION (RICHARDSON AND WILES, 1990)

DR_s	DURABILITY DESCRIPTION
0 - 50	Shale can be considered soil-like, nondurable
50 - 70	Shale is of intermediate behavior, hard and nondurable, more difficult to excavate and break down during compaction.
70 - 90	Shale tends to be hard and more durable. Can be rock-like but should not be considered so.
90 - 100	Truly rock-like shales, durable DR_s limit not well defined at present.

TABLE 3 UNDERCLAY/CLAYSTONE MOISTURE CONTENT DATA FRO SUBSIDENCE AREA IN SOUTHERN ILLINOIS (MARINO ET AL, 1980).

BORING	ROCK	DEPTH BELOW COAL	LOCATION	MOISTURE CONTENT	CORE RECOVERY (IN UNDERCLAY/ CLAYSTONE)	COMMENTS
B-1	UNDERCLAY/ CLAYSTONE	0.46 m	Below failed coal rib	9.9%	90%	No significant core loss of underclay/ claystone
B-2	Same, but limey	0.46 m	Below room adjacent to coal pillar	11.7%	33%	Wash out of soft underclay/ claystone core
B-4	Same, but limey	0.85 m	Below room	11.7%	58%	Wash out of soft underclay/ claystone core
B-5	Same	~1.0 m	Below room	16.5%	~40%	Wash out of soft underclay/ claystone core

TABLE 4 VERTICAL SWELL AND OSR (1/4 pt) VALUES FOR UNDERCLAY/CLAYSTONE BELOW HERRIN COAL IN MINE ROOMS (SEE FIGURE 14).

HOLE	E	W_r	d_r/W_r	ε_r	OSR (1/4 pt)
B-5	61%	6.86 m	0.09	29%	0.023
			0.13	7%	0.057
B-6	65%	5.09 m	0.16	28%	0.106
			0.17	10%	0.122
			0.19	25%	0.155
			0.20	21%	0.172
			0.20	17%	0.172

---

where:

ε_r	=	vertical swell	S	=	saturation
	=	$(e_f - e_0)/(1 + e_0)$		=	100% (assumed)
e_0	=	initial void ratio	G	=	specific gravity
e_f	=	final void ratio		=	2.7 (assumed)
e	=	(MC•G)/S	MC	=	moisture content

TABLE 5 SOFTENED FLOOR BEARING CAPACITY IN PERCENT OF UNSOFTENED CAPACITY, RQR.

W_p / W_r \ W_p / h_t	1	2.5	5.0
1	22%	57%	–
1.66	–	–	56%
2	14%	46%	38%
4	22%	33%	35%
6	42%	33%	31%
10	53%	42%	32%

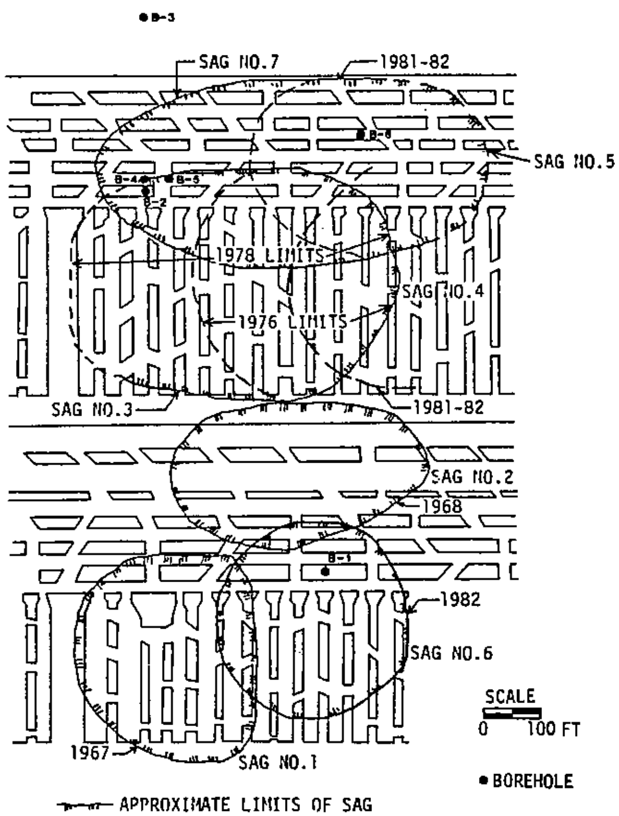

FIGURE 1 SUBSIDENCE OVER THE MINED-OUT AREAS IN DANVILLE, ILLINOIS (MARINO, 1990)

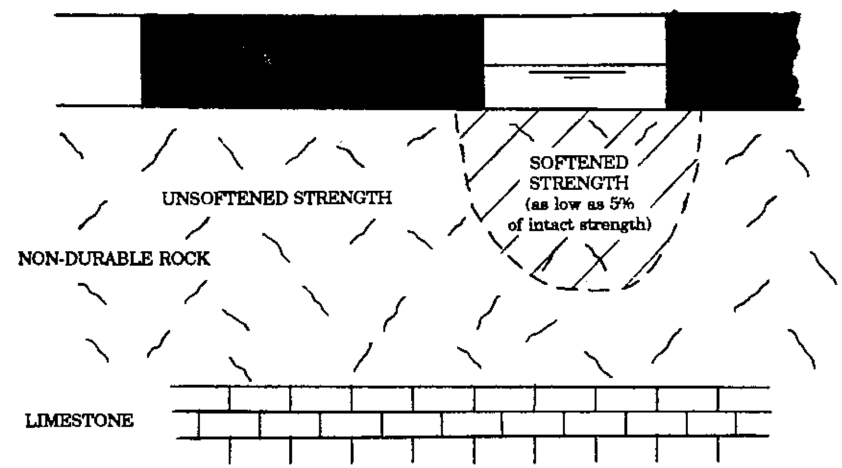

FIGURE 2 CONCEPTUAL SKETCH OF THE INITIAL ZONE OF SOFTENING IN NON-DURABLE FLOOR MATERIALS

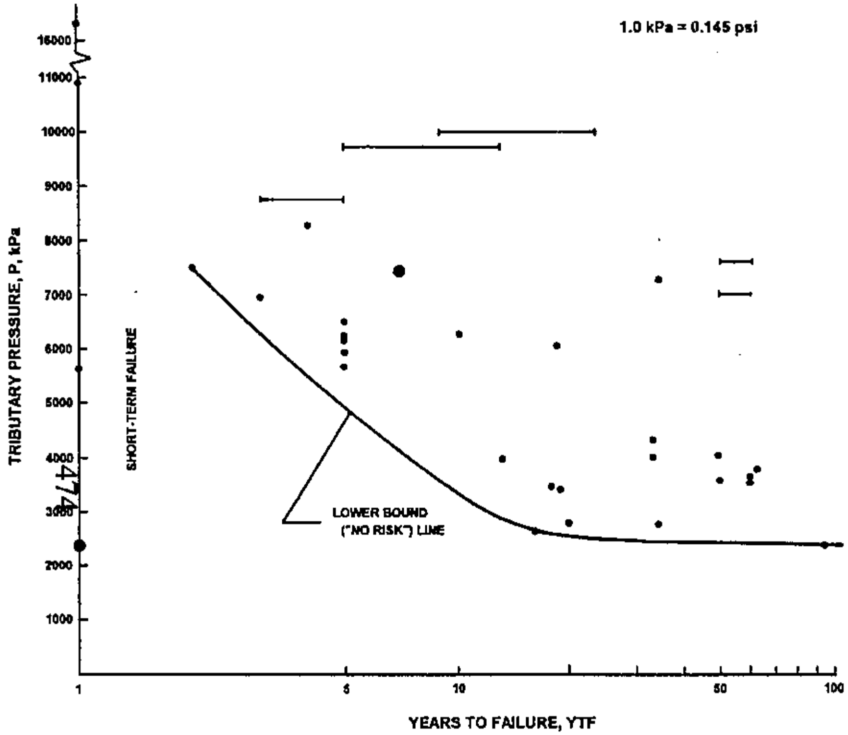

FIGURE 3 TRIBUTARY PRESSURES PLOTTED AGAINST YEARS TO FAILURE FOR CASE DATA (MARINO AND BAUER, 1990)

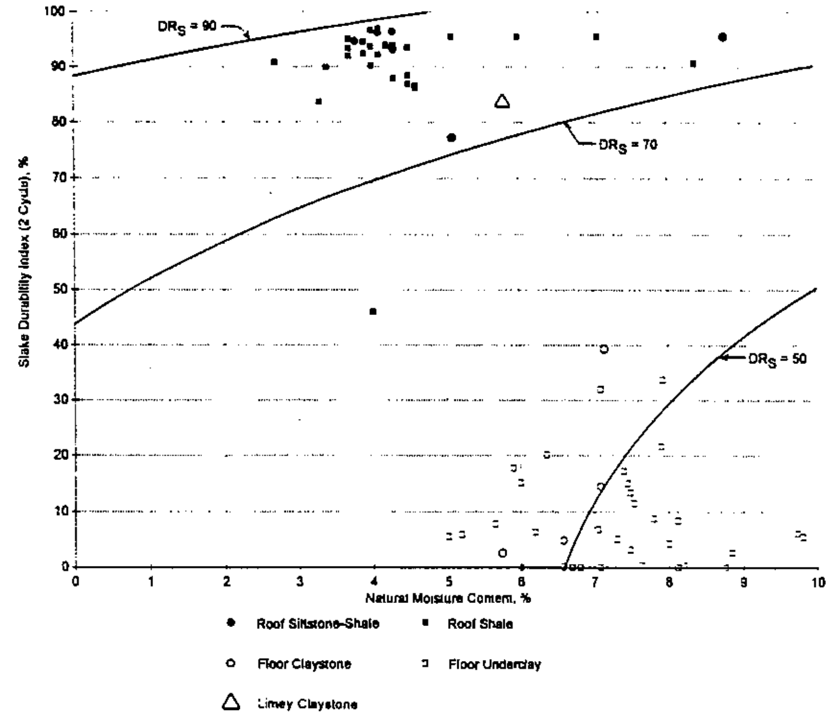

FIGURE 4 DURABILITY CLASSIFICATION OF COAL MINE MATERIALS FROM AN INDIANA MINE (AFTER RICHARDSON AND WILES, 1990)

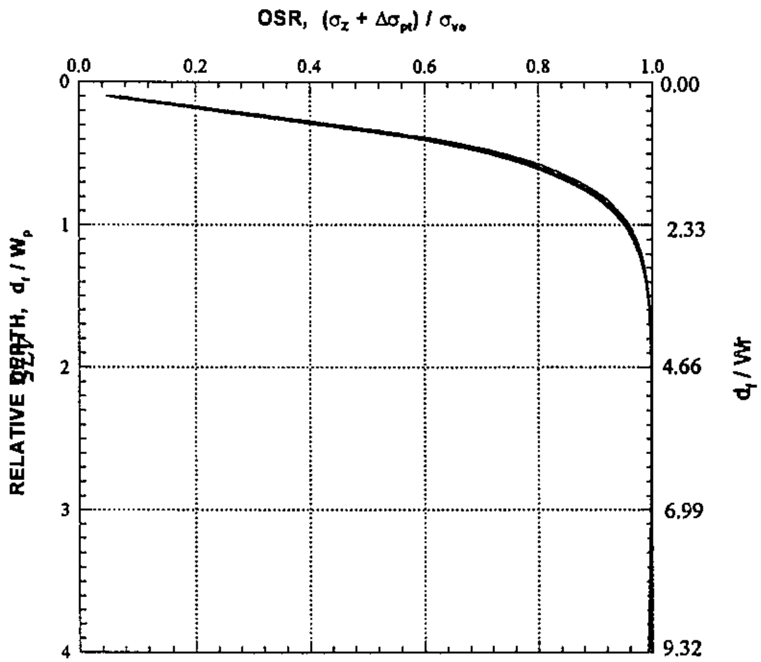

FIGURE 5 OSR PLOTTED AGAINST d_f/W_r FOR A POINT IN THE MIDDLE OF ROOM FOR STRIP PILLARS WITH D/W_r RANGING FROM 10 TO 1000 AT AN EXTRACTION RATIO OF 30%

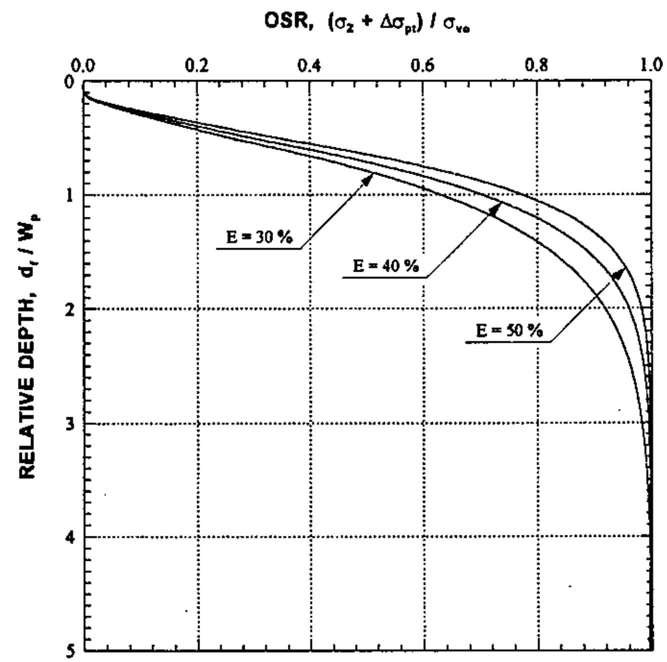

FIGURE 6 OSR PLOTTED AGAINST d_f/W_r FOR A POINT IN THE MIDDLE OF ROOM FOR STRIP AND MID-SQUARE PILLARS FOR EXTRACTION RATIOS OF 30, 40 AND 50%.

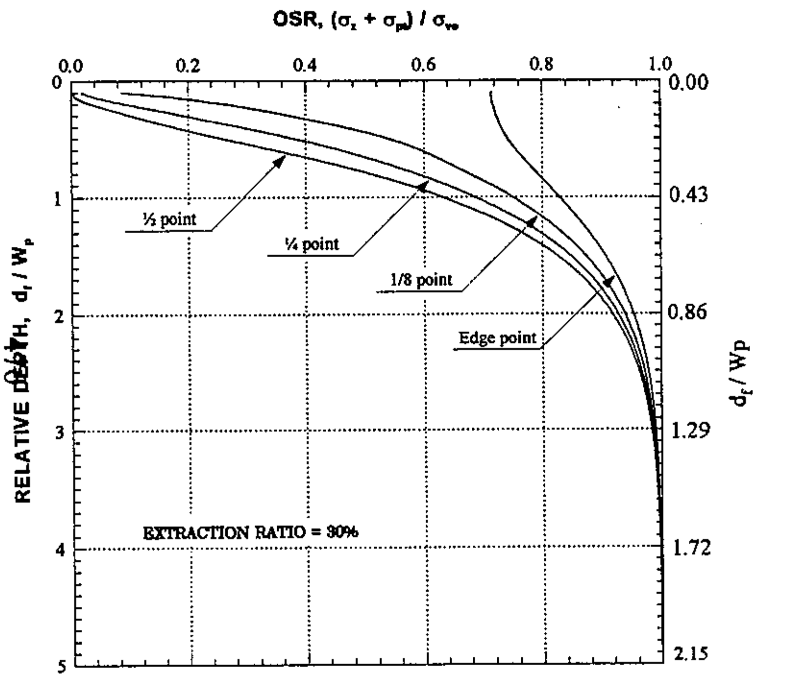

FIGURE 7 OSR PLOTTED AGAINST d_f/W_r FOR POINTS AT PILLAR EDGE, AS WELL AS AT 1/8, 1/4 AND 1/2 ROOM WIDTH FROM PILAR AT AN EXTRACTION RATIO OF 30% (STRIP AND MID-SQUARE PILLARS).

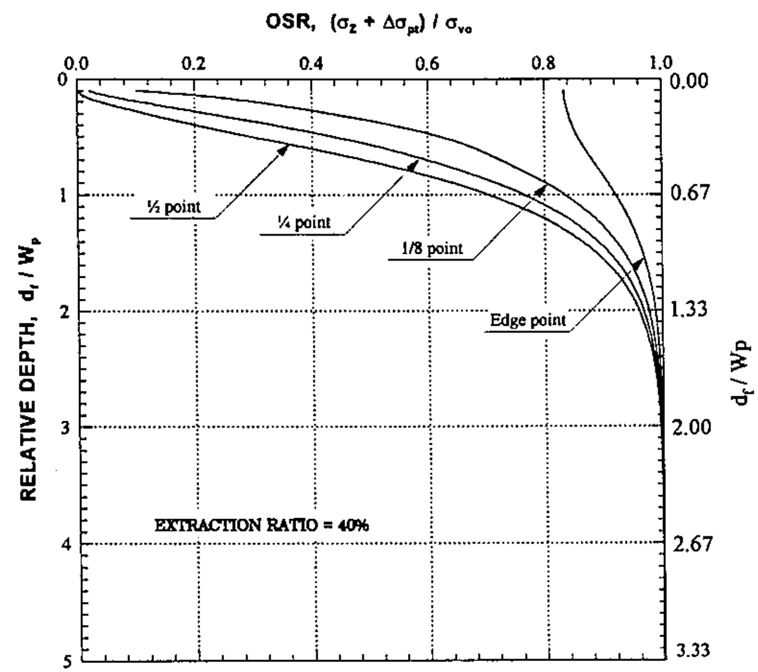

FIGURE 8 OSR PLOTTED AGAINST d_f/W_r FOR POINTS AT PILLAR EDGE, AS WELL AS AT 1/8, 1/4 AND 1/2 ROOM WIDTH FROM PILLAR AT AN EXTRACTION RATIO OF 40% (STRIP AND MID-SQUARE PILLARS).

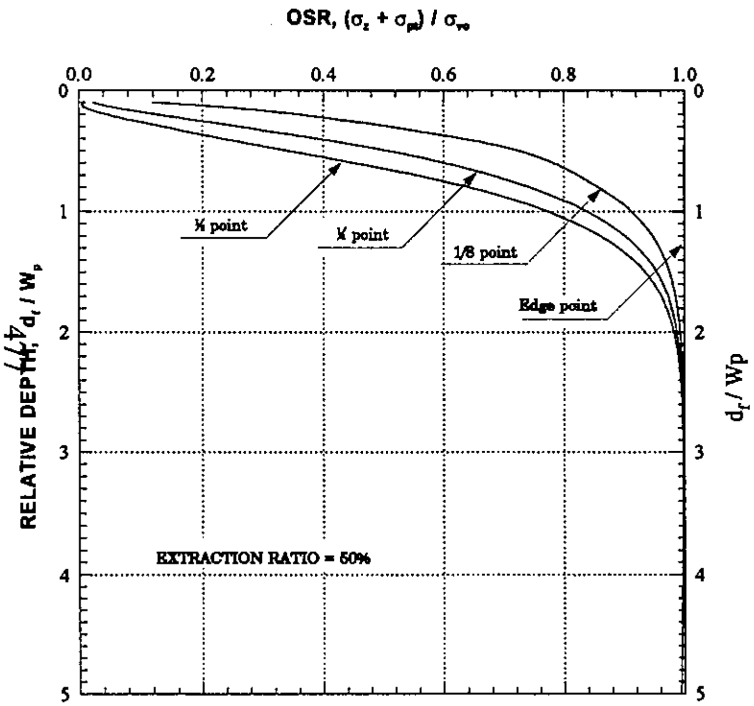

FIGURE 9 OSR PLOTTED AGAINST d_f/W_r FOR POINTS AT PILLAR EDGE, AS WELL AS AT 1/8, 1/4 AND 1/2 ROOM WIDTH FROM PILLAR AT AN EXTRACTION RATIO OF 50% (STRIP AND MID-SQUARE PILLARS).

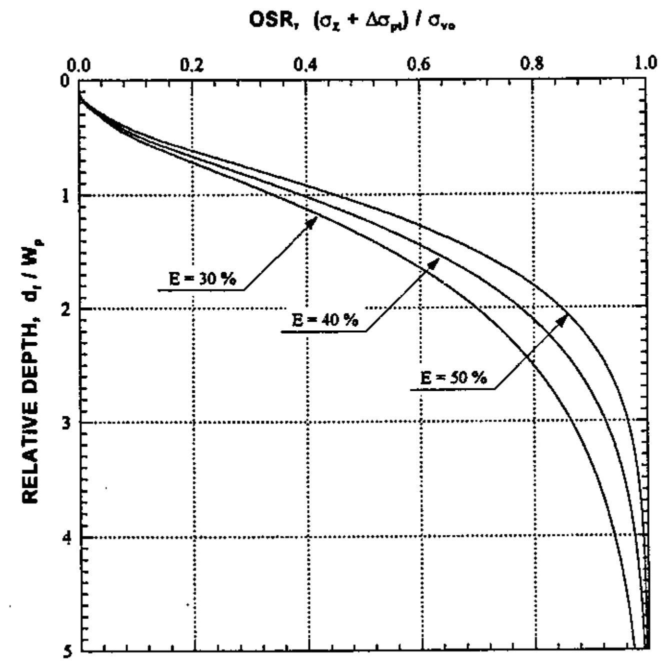

FIGURE 10 OSR PLOTTED AGAINST d_f/W_r FOR A POINT IN THE MIDDLE OF THE ROOM INTERSECTION FOR A SQUARE PILLAR GEOMETRY FOR EXTRACTION RATIOS OF 30, 40 AND 50%.

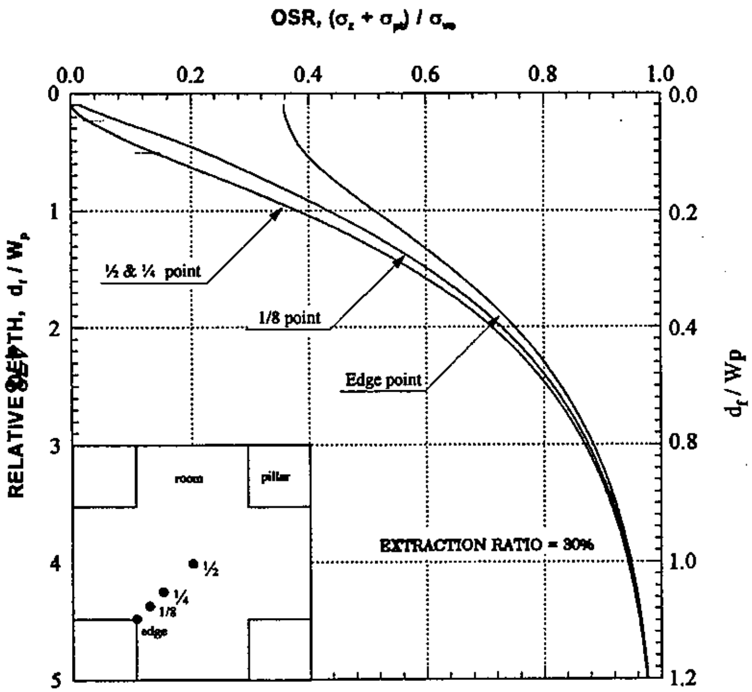

FIGURE 11 OSR PLOTTED AGAINST d_f/W_r FOR POINTS AT THE CORNER OF A SQUARE PILLAR, AS WELL AS AT 1/8, 1/4 AND 1/2 THE DIAGONAL DISTANCE ACROSS THE ROOM INTERSECTION FOR AN EXTRACTION RATIO OF 30% (SQUARE PILLARS).

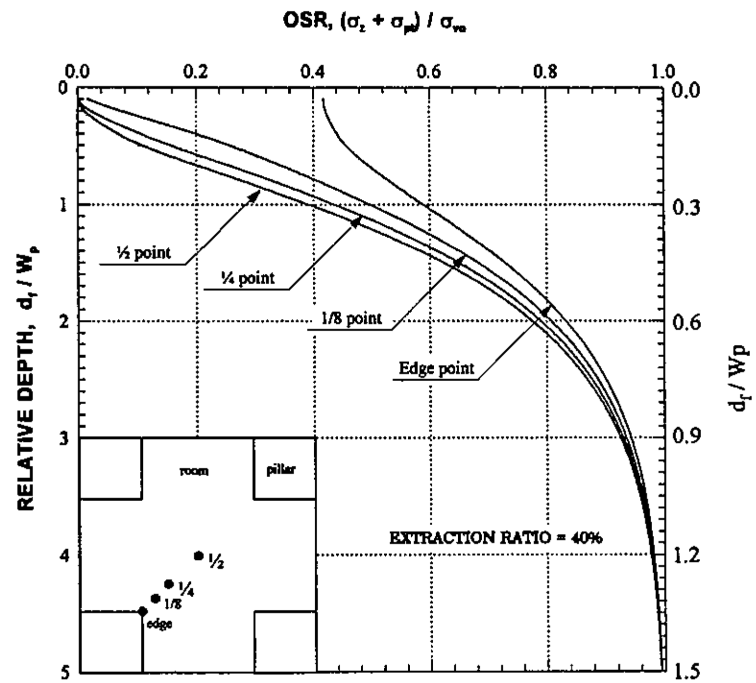

FIGURE 12 OSR PLOTTED AGAINST d_f/W_r FOR POINTS AT THE CORNER OF A SQUARE PILLAR, AS WELL AS AT 1/8, 1/4 AND 1/2 THE DIAGONAL DISTANCE ACROSS THE ROOM INTERSECTION FOR AN EXTRACTION RATIO OF 40% (SQUARE PILLARS).

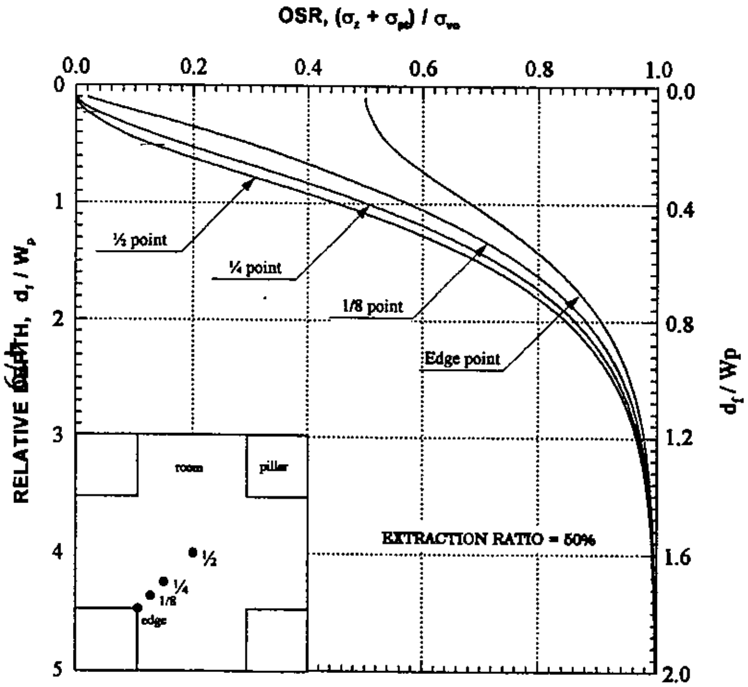

FIGURE 13 OSR PLOTTED AGAINST d_f/W_r FOR POINTS AT THE CORNER OF A SQUARE PILLAR, AS WELL AS AT 1/8, 1/4 AND 1/2 THE DIAGONAL DISTANCE ACROSS THE ROOM INTERSECTION FOR AN EXTRACTION RATIO OF 50% (SQUARE PILLARS).

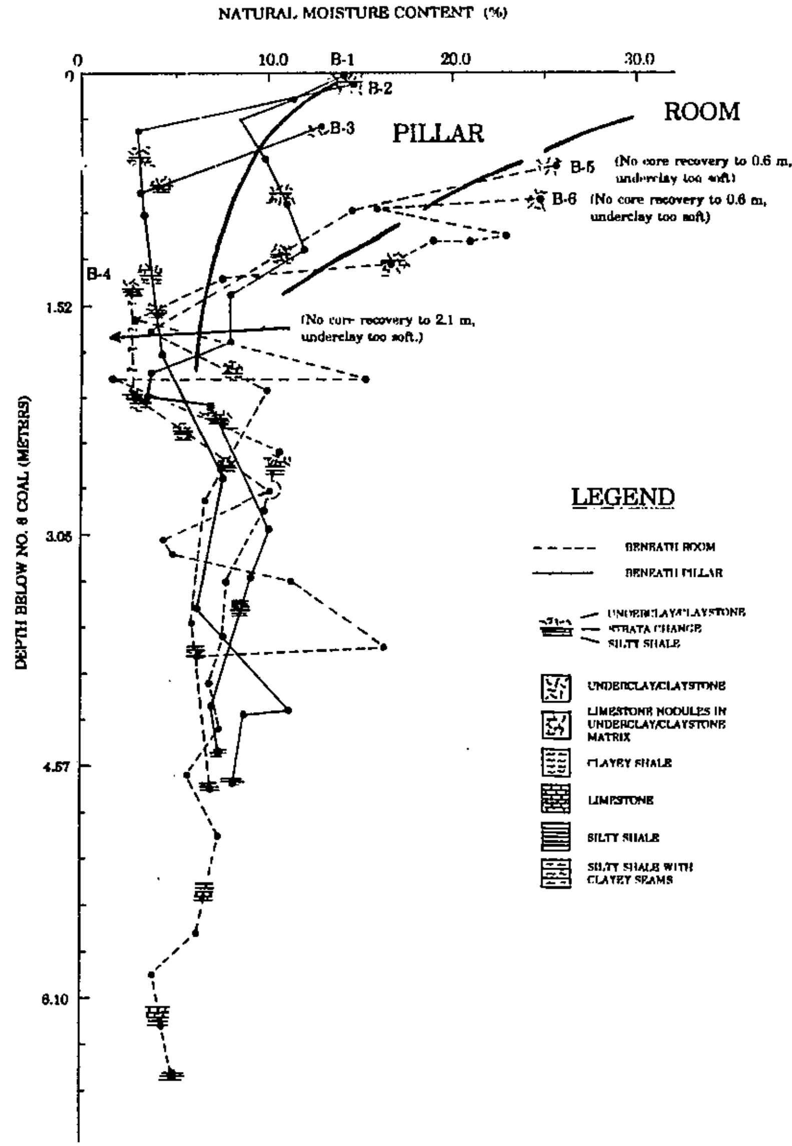

FIGURE 14 MOISTURE CONTENT PROFILES FOR FLOOR STRATA BENEATH PILLARS AND ROOMS FOR MINE IN NO. 6 COAL SEAM NEAR DANVILLE, ILLINOIS (MARINO ET AL, 1982, AND MARINO AND DEVINE, 1985).

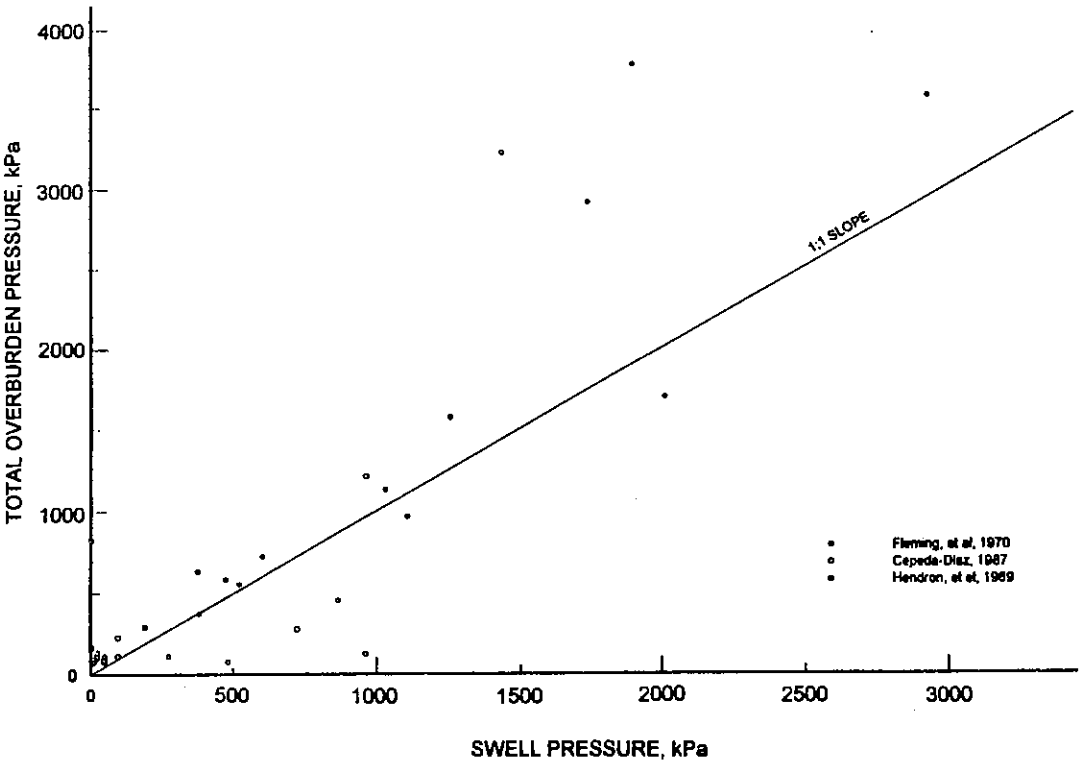

FIGURE 15 TOTAL OVERBURDEN PRESSURE VERSUS SWELL PRESSURE FOR SHALE SAMPLES.

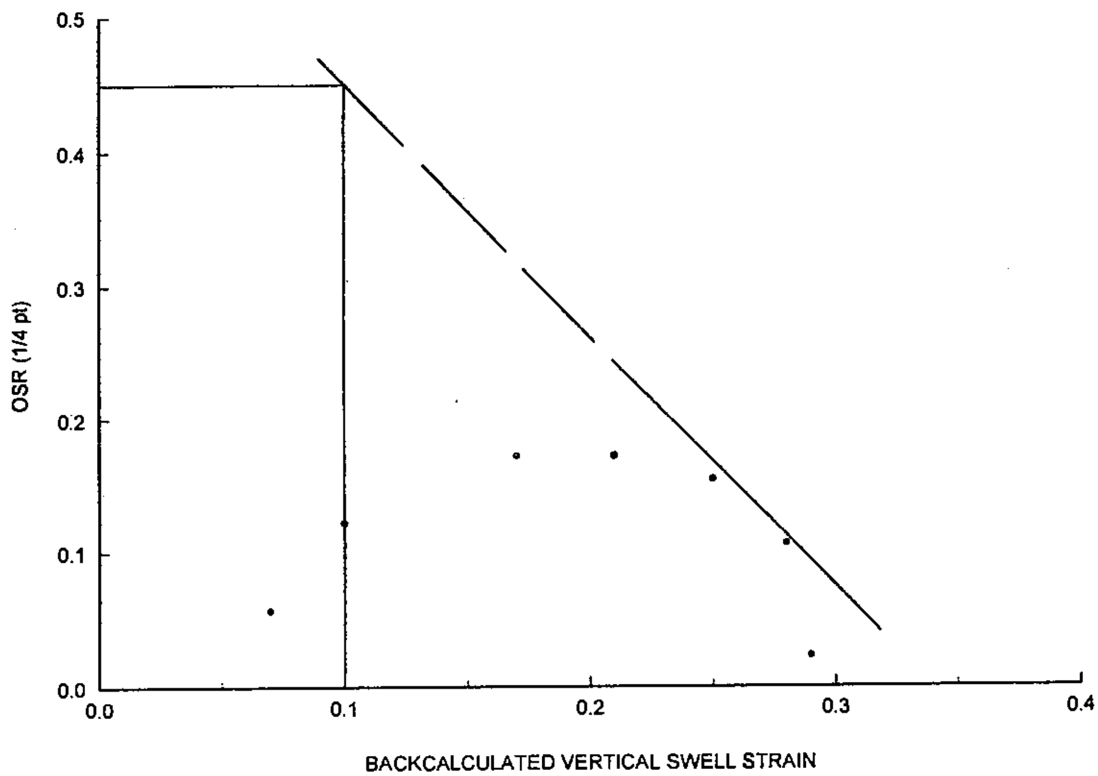

FIGURE 16 BACKCALCULATED SWELL STRAINS IN THE MINE ROOM VERSUS OSR FOR UNDERCLAY/CLAYSTONE.

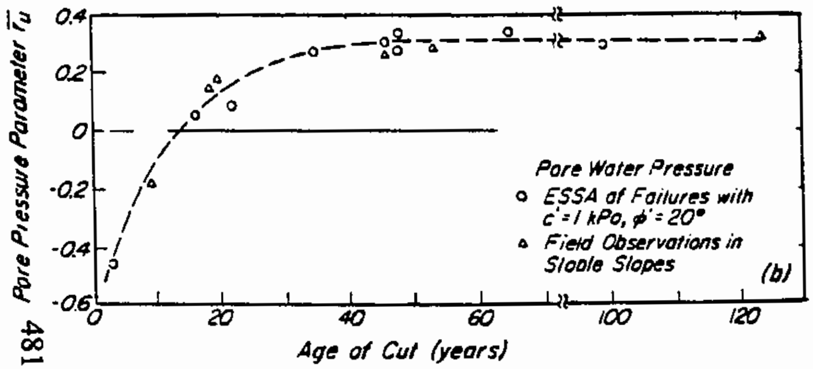

where: $\bar{r}_u$ = average value of r_u = total porewater pressure / total overburden pressure

FIGURE 17 LONG-TERM BEHAVIOR OF CUTS IN LONDON CLAY. RELATION BETWEEN POREWATER PRESSURE PARAMETER r_u AND AGE OF CUT (MESRI ET AL, 1996 AFTER SKEMPTON 1977, CHANDLER 1988).

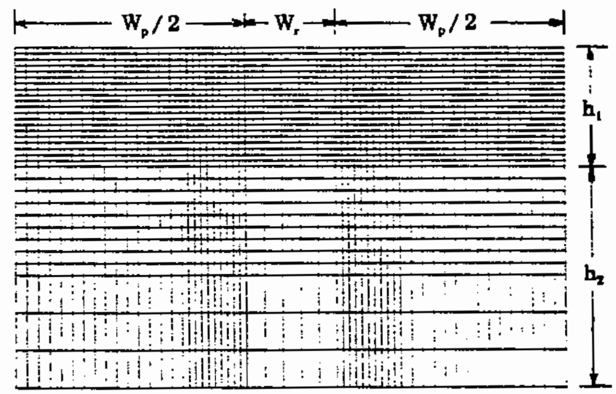

where: W_p = width of pillar

W_r = width of room

h_1 = underclay-claystone thickness

h_2 = durable shale thickness

FIGURE 18 SAMPLE FEM MESH USED TO ANALYZE ULTIMATE BEARING CAPACITY OF FLOOR.

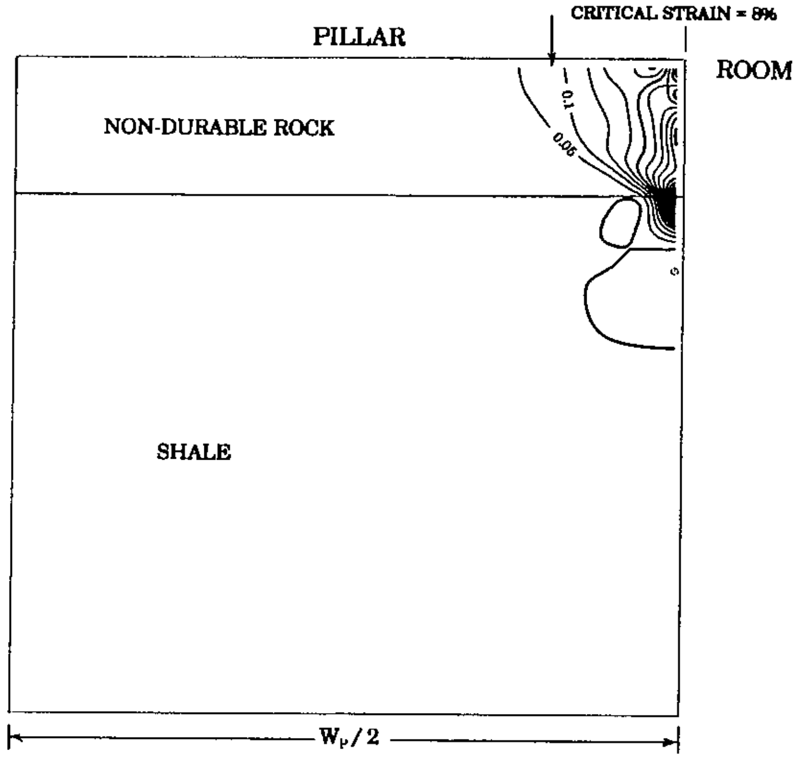

FIGURE 19 AN EXAMPLE PLOT OF THE OCTAHEDRAL SHEAR STRAIN BENEATH THE PILLAR FOR W_p/W_r = 2.5 AND W_p/h_1 = 10 AT 1.18 CM VERTICAL DISPLACEMENT.

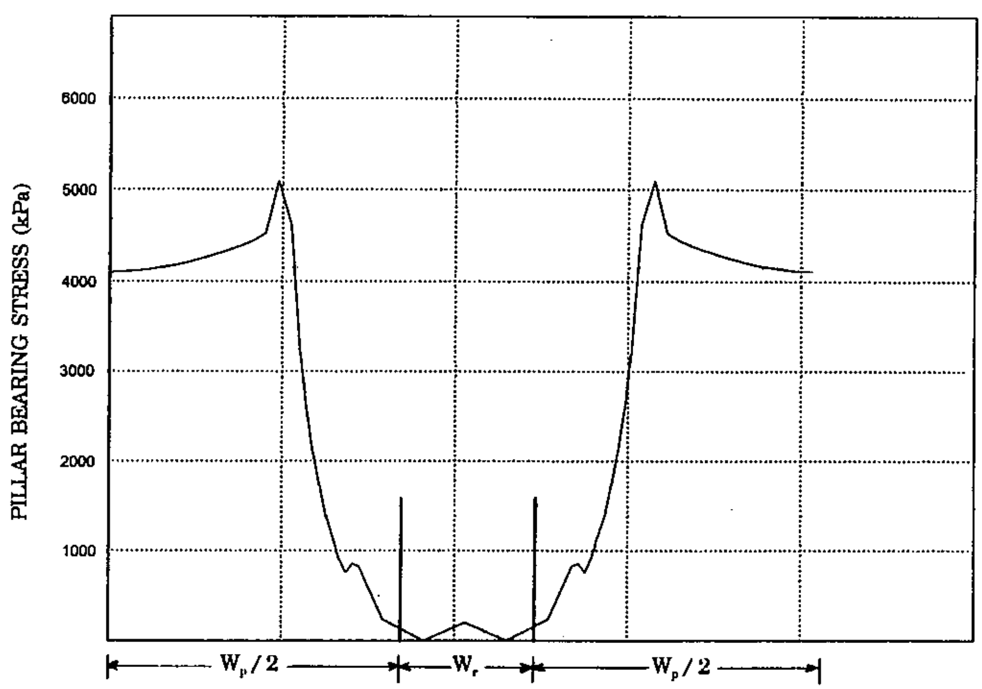

FIGURE 20 AN EXAMPLE PLOT OF THE VERTICAL BEARING PRESSURE ALONG THE PILLAR FOR W_p/W_r = 2.5 AND W_p/h_1 = 10 AT 1.18 CM VERTICAL DISPLACEMENT (SAME CASE AS IN FIGURE 19).